

POLYGONAL SYMPLECTIC BILLIARDS

PETER ALBERS, GAUTAM BANHATTI, FILIP SADLO, RICHARD SCHWARTZ,
AND SERGE TABACHNIKOV

ABSTRACT. In this article, we study polygonal symplectic billiards. We provide new results, some of which are inspired by numerical investigations. In particular, we present several polygons for which all orbits are periodic. We demonstrate their properties and derive various conjectures using two numerical implementations.

1. INTRODUCTION

Planar symplectic billiard is a discrete-time dynamical system on oriented chords of a piecewise smooth convex closed curve (billiard table) in the plane depicted in Figure 1. Symplectic billiards were introduced by Albers and Tabachnikov [1]. The name symplectic billiards is due to the fact that they can be defined in linear symplectic space. In the plane, symplectic billiards commute with affine transformations.

A symplectic billiard table may be a polygon. In this case, the reflection is not defined if the head of an oriented chord is a vertex of the polygon or when the head and the tail of an oriented chord belong to parallel sides. In this article, we only consider convex polygons, (even though symplectic billiards can also be defined on non-convex polygons).

So far, two classes of polygons were considered [1], affine-regular polygons and trapezoids. In both cases, all symplectic billiard orbits are periodic. In this paper, we describe other families of polygons with this property. We call them periodic polygonal symplectic billiards.

Let us briefly mention two other, much better known, classes of polygonal billiards: Euclidean billiards and outer billiards (see, e.g., the book [3] for a survey). In the former billiards, periodic trajectories appear in 1-parameter families of mutually parallel trajectories, but trajectories with different initial directions, no matter how close, will eventually diverge and hit different sides of the polygon. The celebrated Ivrii conjecture states that the set of periodic orbits of a planar billiard has zero phase area. However, the example of an equilateral right spherical triangle shows that in spherical geometry billiards all of whose orbits are closed exist. Moreover, in outer billiards, which is played outside of the curve, it is possible for all trajectories to be periodic: this happens for all lattice polygons, see again the book [3].

In this article some of our results are proof-based while others are driven by numerical experiments. Based on that we formulate several conjectures. For our numerical investigations we utilized two research codes developed in the context of this paper, one for effective determination of periodicity and one for interactive exploration of phase-space structure. Beyond that we only aware of implementations in this field by Boshe-Ploes et al. [6] and Raymond Friend in his honors thesis at Pennsylvania State University.

Date: December 20, 2019.

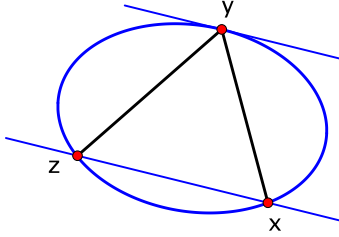


Figure 1. *The symplectic billiard reflection: xy reflects to yz if xz is parallel to the tangent line of the curve at point y .*

2. GENERAL FACTS ABOUT POLYGONAL SYMPLECTIC BILLIARDS

In this section, we recall known and prove some new facts about polygonal symplectic billiards.

2.1. Phase space and phase area.

Let \mathbf{P} be an n -gon with vertices P_1, P_2, \dots, P_n , oriented counterclockwise. We define the vectors $v_i = P_{i+1} - P_i$, where the indices are understood cyclically and denote by $v_i \times v_j$ the set of chords whose tail is in the interior of the side $P_i P_{i+1}$ and whose head is in the interior of the side $P_j P_{j+1}$. We use bracket $[\cdot, \cdot]$ to denote the determinant of two vectors.

Let T be the symplectic billiard map defined as in Figure 1. It is piecewise continuous. Its phase space is the union of the sets $v_i \times v_j$, $i, j = 1, \dots, n$, with $i \neq j$ and v_i and v_j not being parallel. After parameterizing the perimeter of \mathbf{P} , the phase space is represented by a square, tiled by the rectangles $v_i \times v_j$. The rectangles $v_i \times v_j$ with v_i and v_j being parallel, along with the squares $v_i \times v_i$, are excised (they are represented by black squares in the pictures below). In this representation, the first coordinate describes the position of the tail of a chord, and the second coordinate the position of its head. The map T is continuous in each rectangle $v_i \times v_j$, see Lemma 2.1.

The phase space has an involution that reverses the direction of a chord. This “time reversal” involution conjugates T and T^{-1} . We reduce the phase space by half by considering only the rectangles $v_i \times v_j$ with $[v_i, v_j] > 0$ and denote this space by $\Phi_{\mathbf{P}}$. Further, define a piece-wise constant area form on the phase space by declaring that the total area of a rectangle $v_i \times v_j$ is $[v_i, v_j]$. We parametrize each side by arc-length and denote the corresponding coordinates by x, y, z etc. Then, if α is the angle between v_i and v_j , and dx and dy are the respective oriented length elements on these sides, then the area form equals $\sin \alpha \, dx \wedge dy$.

Lemma 2.1. *The map T is area preserving. It has the form*

$$T : (x, y) \mapsto (y, z = ax + b), \quad x \in P_i P_{i+1}, y \in P_j P_{j+1}, z \in P_k P_{k+1},$$

with $a = -\frac{\sin \alpha}{\sin \beta}$ and b depending on i, j, k (but not on y), see Figure 2.

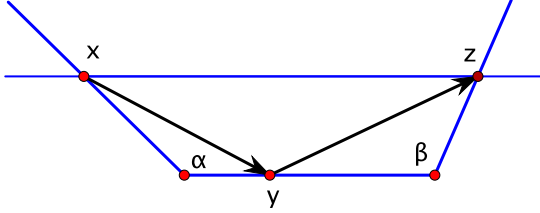


Figure 2. *Distortion of length under projection, see Lemma 2.1.*

Proof. Consider an instance of a reflection, Figure 2. The projection of the i th side on the k th side along the j th side reverses the orientation. This projection is an affine map $x \mapsto z$ that does not depend on y , as long as y stays on the j th side. The projection distorts the length by the ratio $\sin \alpha / \sin \beta$, namely, $\sin \alpha dx = -\sin \beta dz$. It follows that $\sin \alpha dx \wedge dy = \sin \beta dy \wedge dz$, as needed. \square

Remark 2.1. The phase space of polygonal symplectic billiards has a T -invariant area form ω and a T -invariant 2-web of vertical and horizontal lines. These two structures determine a sign-indefinite quadratic form as follows. Given a vector V , let V_1 and V_2 be its horizontal and vertical components with respect to the 2-web, and set $g(V) = \omega(V_1, V_2)$. We obtain a pseudo-Euclidean metric g , and it follows that T is a piecewise isometry relative to this pseudo-Euclidean metric.

We now give another interpretation of the phase area. Denote by $-\mathbf{P}$ the reflection of \mathbf{P} about the origin. Then the *difference body* $D(\mathbf{P})$ of a convex body \mathbf{P} is the Minkowski sum of \mathbf{P} with $-\mathbf{P}$. In other words, the difference body is centered at the origin and is formed by the vectors that connect pairs of points of \mathbf{P} . For example, the difference body of a triangle is an affine-regular hexagon, and the difference body of a square is a square twice as large.

Let \mathbf{P} be a convex plane polygon, the symplectic billiard table. This induces a map $f : \Phi_{\mathbf{P}} \rightarrow D(\mathbf{P})$ that sends chords of \mathbf{P} to points of its difference body. We equip the latter with the area form induced from that in the plane.

Lemma 2.2. *The map f is an area-preserving bijection of the interior of $\Phi_{\mathbf{P}}$ to an open dense subset of $D(\mathbf{P})$.*

Proof. Let us construct an inverse of the map f on an open dense part of $D(\mathbf{P})$. For this we assume for the moment that \mathbf{P} is strictly convex with smooth boundary γ , oriented counter-clockwise. An affine diameter of \mathbf{P} is a chord of γ with parallel tangent lines at its end points.

Let vector w be a nonzero vector in the interior of $D(\mathbf{P})$. We would like to represent w as the vector AB , where $A \neq B$ are in the interior of \mathbf{P} . If one, or both, points A, B lie on γ , one can parallel-translate the segment AB so that both points are inside \mathbf{P} . Indeed, the only situation when such a translation does not exist, is when AB is an affine diameter of \mathbf{P} , as illustrated in Figure 3. But, then w would lie on the boundary of the difference body, the case that we already excluded.

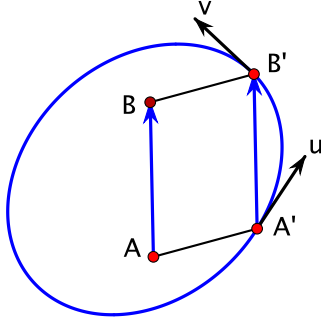


Figure 3. *Moving a vector to the boundary.*

Consider the oriented line through AB and move it to the right (with respect to the orientation of the plane). By continuity and strict convexity, there will be a unique moment when the intersection points, A', B' , of the moving line with γ are such that $A'B' = w$. Let u and v be the oriented tangent vectors of γ at A' and B' . We claim that $[u, v] \neq 0$. Indeed, if $[u, v] = 0$, then either $v = u$ or $v = -u$. In the former case, $B' = A'$ and $w = 0$, and in the latter case, $A'B' = AB$ is an affine diameter. Both cases are excluded. The punctured interior of $D(\mathbf{P})$ is connected, hence $[u, v]$ has a constant sign, and it is easy to see that it is positive (see Figure 3). Thus, $A'B' \in \Phi_{\mathbf{P}}$, and the map $w \mapsto A'B'$ is the inverse of f .

If \mathbf{P} is a convex polygon, the same construction applies with the following adjustments. In addition to the boundary of $D(\mathbf{P})$ and the origin, we also remove from it the vectors that are equal to tv_i for some index i and $t \in [0, 1]$, the vectors whose endpoints are on parallel sides of \mathbf{P} (if any), and the vectors for which point A' or B' is a vertex of the polygon. These sets are 1-dimensional, and f is a bijection of the interior of $\Phi_{\mathbf{P}}$ to their complement.

Concerning the area-preserving property, let x and y be arc length parameters on the sides on which points A' and B' lie, and let u and v be the unit orienting vector along these sides, respectively. Then, locally, the map f is given by $(x, y) \mapsto yv - xu \in \mathbb{R}^2$. The induced area form is $[u, v]dx \wedge dy$, as needed. \square

Remark 2.2. The total phase space area of the symplectic billiard in a strictly convex plane domain with smooth boundary equals the area of its difference body, [1]. The proof involves manipulations with the support function of the body.

2.2. Symbolic dynamics and tiles.

As before, we label the sides of the polygon $1, \dots, n$, and assign to each orbit of the symplectic billiard map T its symbolic orbit, the bi-infinite sequence of the labels of the sides that are visited by the orbit. A periodic billiard orbit has a periodic symbolic orbit.

Define a *tile* as the set of phase points with the same periodic symbolic orbit. The *discontinuity set* consists of the phase points for which some iteration of T , in the future or in the past, is not defined, that is, whose orbit ends up at a vertex or starts at a vertex of the polygon. The set of chords, one of whose endpoints is a vertex and another

lies on a side, is either a horizontal or a vertical segment. Lemma 2.1 implies that the discontinuity set is a union of horizontal and vertical segments. Thus, its complement is the union of tiles.

Lemma 2.3. *The tiles are phase rectangles, possibly degenerate (segments or points). In particular, every tile is connected.*

If a tile is a genuine rectangle, that is, has a positive phase area, then its symbolic orbit is periodic. Furthermore, every orbit in this tile is periodic. More precisely, let M be a tile of positive area with a periodic symbolic orbit of period n . Then T^n maps M to itself, and the return map T^n has either order 4, or order 2, or it is the identity.

Proof. Let $(\dots, i_0, i_1, i_2, \dots)$ be a symbolic orbit. The phase points with the symbolic coding (i_0, i_1) form the set $v_{i_0} \times v_{i_1}$, the points with the coding (i_0, i_1, i_2) form the set $(v_{i_0} \times v_{i_1}) \cap T^{-1}(v_{i_1} \times v_{i_2})$, and so on. The preimages and images of rectangles with vertical and horizontal sides are rectangles with vertical and horizontal sides, and the intersection of a finite number of such rectangles is again a rectangle of this kind, cf. Lemma 2.1. An infinite intersection is still a rectangle, possibly a degenerate one.

Assume that a tile M has positive area. Since the total phase area is finite and T is area preserving, there exist $i > j$ such that the tiles $T^i(M)$ and $T^j(M)$ intersect. Hence, $T^{i-j}(M)$ intersects M , and since M is a tile, it follows that $T^{i-j}(M) = M$. Therefore the symbolic orbit of M is $(i - j)$ -periodic. The tile M is a rectangle, and the return map T^{i-j} is an orientation-preserving affine isomorphism of this rectangle. Hence, this map is conjugated to a rotation of a square through an angle that is a multiple of $\pi/2$, that is, either $\pi/2$ (order 4), or π (order 2), or 2π (the identity). \square

2.3. Periodic trajectories.

Call a periodic trajectory in a polygon \mathbf{P} *stable* if this trajectory persists under every sufficiently small perturbation of \mathbf{P} . For example, the 3-periodic orbits in a triangle that connects the mid-points of its sides is stable, whereas a 4-periodic trajectory in a square is not stable: it can be destroyed by an arbitrary small perturbation of the square.

A periodic trajectory is called *isolated* if its tile has zero area.

Proposition 2.1. *An isolated periodic orbit is stable. In addition,*

- *if n is odd, then an n -periodic orbit is stable. However, it is never isolated, and the return map to its tile has order 4;*
- *if n is even but not divisible by four, then an n -periodic orbit is stable. If it is not isolated, then the return map to its tile has order 2;*
- *if n is divisible by four and the quotient λ , (which is defined in (1) in the proof below) is different from 1, then the respective periodic orbit is stable. If $\lambda = 1$, then the return map of the respective tile is the identity. In this case, as indicated by our numerical experiments, the orbit may be stable or unstable.*

Remark 2.3. The proof of Proposition 2.1 relies on the simple fact that an orbit is stable, if the differential of the return map does not have 1 as an eigenvalue. In our case this map

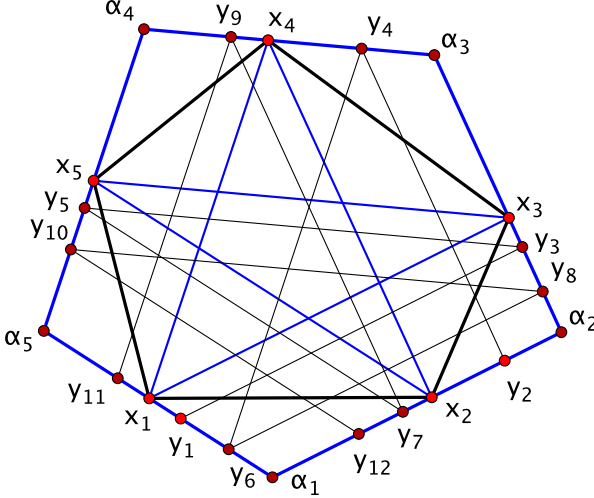


Figure 4. A 5-periodic trajectory x_1, \dots, x_5 and a nearby trajectory y_1, y_2, \dots . Points y_1 and y_{11} are symmetric with respect to point x_1 , and points y_2 and y_{12} are symmetric with respect to point x_2 .

is a composition of rather explicit affine transformations which leads to the description in Proposition 2.1.

Proof. Let x_1, \dots, x_n be a periodic trajectory. For every i , the side L_i containing point x_i is parallel to x_{i-1}, x_{i+1} . Let α_i be the angle between L_i and L_{i+1} .

Let n be odd, and let y_1y_2 be a chord sufficiently close to x_1x_2 . We trace the evolution of odd-numbered and even-numbered points y_i separately. After n reflections, y_1 returns to the line L_1 as y_{1+n} and y_2 returns to the line L_2 as y_{2+n} and similarly after $2n$ reflections, y_1 returns to the line L_1 as y_{1+2n} and y_2 returns to the line L_2 as y_{2+2n} . Each of these return maps reverses the orientation and preserves the length, because the distortion of the length equals

$$\frac{\sin \alpha_1}{\sin \alpha_2} \frac{\sin \alpha_3}{\sin \alpha_4} \dots \frac{\sin \alpha_{2n-1}}{\sin \alpha_{2n}} = 1$$

(every angle appears twice, once in the numerator and once in the denominator). That is, the return maps to the sides L_1 and L_2 are the reflection in points x_1 and x_2 , respectively. See Figure 4.

It follows that the phase point y_1y_2 is $4n$ -periodic. These phase points form a tile, this tile returns to itself after n iterations, and order of the return map T^n is four. The phase point x_1x_2 is the center of this tile, and it is a hyperbolic fixed point of T^n with the eigenvalues $\pm\sqrt{-1}$. A small perturbation of a polygon does not destroy such a fixed point, hence the perturbed polygon also has an n -periodic symplectic billiard trajectory.

Now let $n = 2m$ be even. Arguing in the same way, the first return of point y_1 to line L_1 occurs after n reflections, and likewise for point y_2 .

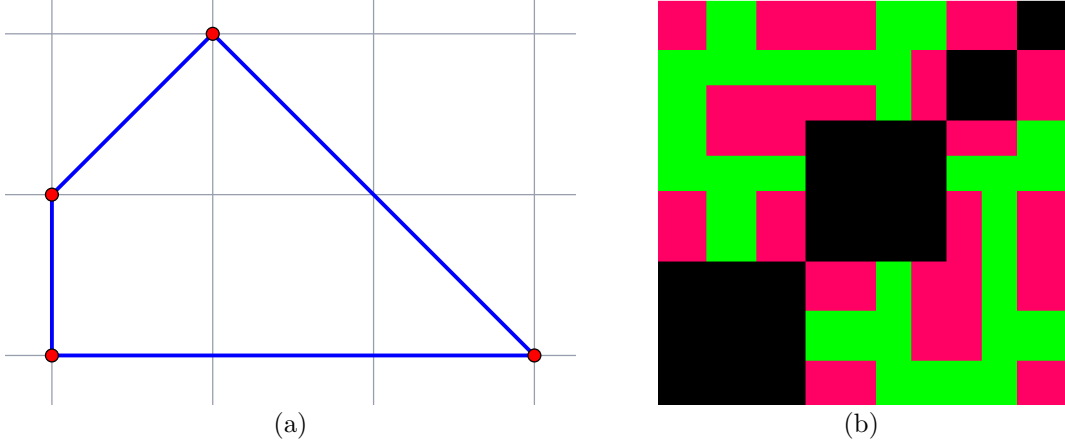


Figure 5. The Quad in configuration space (a) and its phase space (b). Green parts of the phase space are 36-periodic, and the red ones 20-periodic.

The distortion of the length on L_1 equals

$$(1) \quad \frac{\sin \alpha_1}{\sin \alpha_2} \frac{\sin \alpha_3}{\sin \alpha_4} \dots \frac{\sin \alpha_{n-1}}{\sin \alpha_n} =: \lambda,$$

and for L_2 , the distortion equals $1/\lambda$. The orbit is not isolated if and only if $\lambda = 1$, cf. Lemma 2.1.

If m is odd, each of these return maps reverses the orientation of the line, and is a homothety with a negative coefficient. Hence the fixed point persists under a sufficiently small perturbation of the polygon. It follows that the n -periodic orbit is stable. If the orbit is not isolated, and $\lambda = 1$, then the return map of the respective tile is a reflection in a point, that has order two.

If n is a multiple of four and $\lambda \neq 1$, then the respective periodic orbit is hyperbolic, with one attracting and one repelling direction. Therefore it is stable. If $\lambda = 1$, then the return map of the respective tile is the identity. The orbit may be either stable or unstable. \square

3. THE QUAD

The first periodic polygonal symplectic billiard table that we discovered is a quadrilateral that we call *the Quad*, see Figure 5. All phase points are periodic with two periods, 20 and 36. See Figure 5 for the phase space colored according to period. We now analyze the dynamics.

Theorem 3.1. *All orbits in the Quad are periodic with periods 20 and 36. The structure of the orbits of the periodic tiles is as follows.*

- One orbit consisting of the tiles that return to themselves after 10 iterations, with the return map having order 2.
- One orbit consisting of the tiles that return to themselves after 9 iterations, with the return map having order 4.

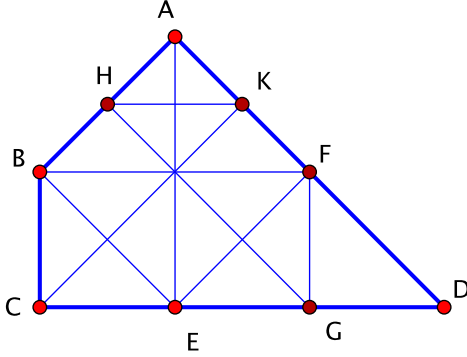


Figure 6. The Quad with marked points on the sides.

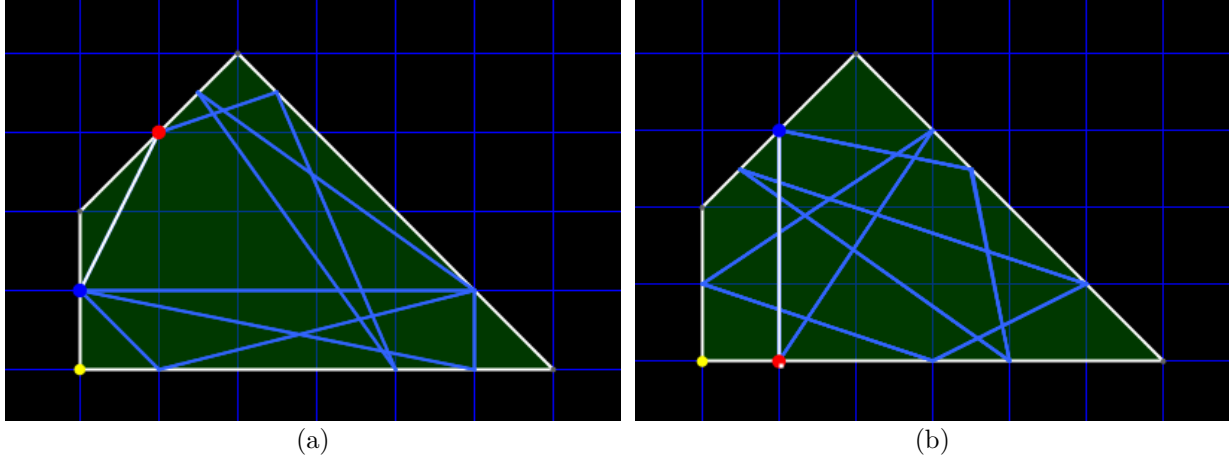


Figure 7. The 10-periodic (a) and 9-periodic (b) trajectories in the Quad.

Proof. Consider Figure 6. We will describe the evolution of two phase rectangles under the symplectic billiard map T , the rectangles $AB \times BC$ and $AB \times CE$.

In the first case, we have

$$\begin{aligned} AB \times BC &\rightarrow BC \times CE \rightarrow CE \times DF \rightarrow DF \times BC \rightarrow BC \times GD \rightarrow GD \times DF \rightarrow \\ &DF \times AH \rightarrow AH \times ED \rightarrow ED \times KA \rightarrow KA \times AB \rightarrow AB \times BC. \end{aligned}$$

Note that the orbit of the rectangle $AB \times BC$ is never split by a discontinuity line, and that it returns to itself after 10 iterations. Following a small segment in $AB \times BC$ reveals that this return map has order two, and its second iteration yields 20-periodic points.

In the second case, we have

$$\begin{aligned} AB \times CE &\rightarrow CE \times FA \rightarrow FA \times BC \rightarrow BC \times EG \rightarrow EG \times DF \rightarrow \\ &DF \times HB \rightarrow HB \times ED \rightarrow ED \times FK \rightarrow FK \times AB \rightarrow AB \times CE. \end{aligned}$$

Once again, the rectangle is never split and it returns back after 9 iterations. As above one sees that the return map has order four, and its fourth iteration yields 36-periodic points.

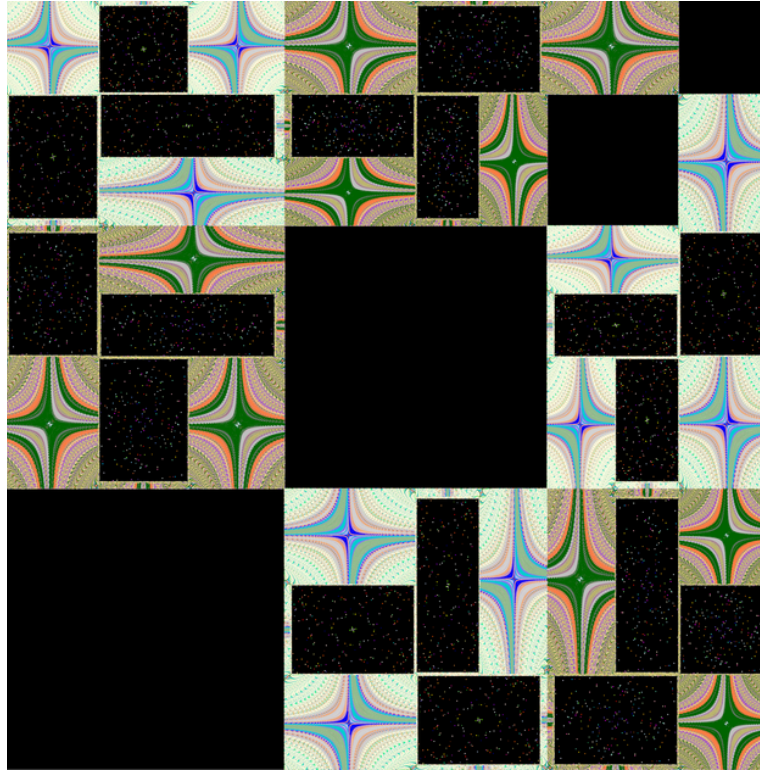


Figure 8. *The phase portrait of a small perturbation of the Quad.*

Assuming that the grid squares in Figure 5 are unit, one calculates the area of the phase space (with respect to the symplectic form on phase space) to be equal to 19, whereas the phase areas of the rectangles $AB \times BC$ and $AB \times CE$ are unit. The orbit of the former rectangle has area 10, and that of the latter has area 9. Hence the whole phase space is tiled by these rectangles, proving that every phase point is either 20- or 36-periodic.

The centers of the rectangles $AB \times BC$ and $AB \times CE$ are, respectively, 10- and 9-periodic trajectories, see Figure 7. \square

Remark 3.1. Figure 8 shows the phase portrait of the symplectic billiard map of a small perturbation of the Quad. In accordance with Proposition 2.1, the 10-periodic tile gives rise to an isolated 10-periodic hyperbolic orbit, whereas the 9-periodic orbit persists and is surrounded by a periodic tile. The points close to the hyperbolic 10-periodic orbit exhibit a kind of slow-fast dynamics. They travel slowly along the hyperbolas while jumping fast between tiles, as is clearly seen in the figure.

4. THE PENTHOUSE

The next periodic polygonal symplectic billiard table in our collection is a pentagon obtained by placing a triangle on top of a parallelogram. Applying an affine transformation, we normalize the parallelogram to be a unit square, and we call the resulting pentagon *the Penthouse* (a pentagon that looks like a house), see Figure 9.

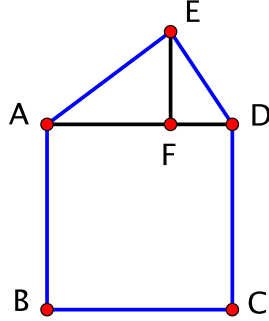


Figure 9. *The Penthouse.*

The affine moduli space of these pentagons is 2-dimensional (while the affine moduli space of all pentagons is 4-dimensional). As parameters (a, b) , one can choose the elevation of the ‘‘roof’’ $a = |EF|$ and its horizontal displacement $b = |AF|$. Then a is a positive real, and $0 < b < 1$. Note that, in the limit $b = 0$ or $b = 1$, we obtain a trapezoid.

A straightforward calculation yields the following result.

Lemma 4.1. *The following table shows 9 rectangles whose union is the phase space together with their phase areas.*

$AB \times BC$	$BC \times CD$	$BC \times DE$	$CD \times DE$	$CD \times EA$
1	1	a	$1 - b$	b

$DE \times EA$	$DE \times AB$	$EA \times AB$	$EA \times BC$
a	$1 - b$	b	a

Recall a result concerning the trapezoids, [1]. Let $u > v$ be the lengths of the parallel sides of a trapezoid. Define its *modulus* as $\lfloor u/(u-v) \rfloor \in \mathbb{Z}$; this is an affine invariant. A trapezoid is *generic* if $u/(u-v) \notin \mathbb{Z}$. The result that we need is as follows: *all orbits in a trapezoid are periodic, and if the modulus of a generic trapezoid is m , then the periods are $16m - 4$, $16m + 4$, and $16m + 12$.*

Define the modulus of a Penthouse similarly:

$$m = \left\lfloor \frac{a+1}{a} \right\rfloor.$$

When a Penthouse degenerates to a trapezoid, its modulus becomes that of the trapezoid. A generic Penthouse is defined similarly: $\frac{a+1}{a}$ is not an integer. We call a Penthouse *tall* if $a > 1$, that is, if $m = 1$.

Conjecture 4.1. *All orbits in a generic Penthouse are periodic with the periods equal to $16m - 4$, $16m + 4$, and $16m + 12$, in particular, the periods do not change if one moves the roof horizontally (but the symbolic orbits may change). Under the bifurcation $m \mapsto m + 1$, the tiles with the largest period $16m + 12$ survive and become the tiles with the smallest period $16m + 12 = 16(m + 1) - 4$; the tiles with the periods $16m - 4$ and $16m + 4$ die and the tiles with periods $16m + 20$ and $16m + 28$ are born.*

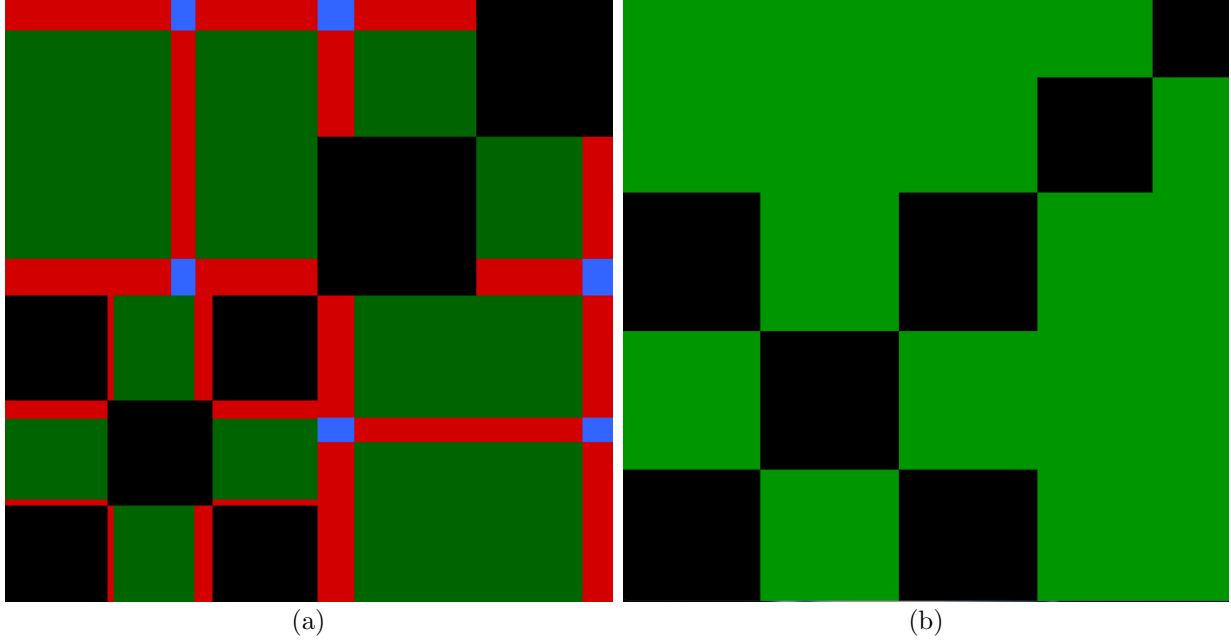


Figure 10. The phase space of a tall Penthouse (a) and at the first bifurcation case $a = 1$ (b). The blue points have period 12, the red ones period 20, and the green ones period 28.

Remark 4.1. We point out that, if Conjecture 4.1 is correct, then there are infinitely many bifurcations as $a \rightarrow 0$ and there three different periods go to infinity. In contrast, the limiting geometric object is a square for which the symplectic billiard map is periodic with one period being 4.

For a tall Penthouse, we provide a complete analysis of the dynamics similar to the one given for the Quad. We also examine the first bifurcation case, i.e., $a = 1$.

Theorem 4.2. All orbits in a tall Penthouse are periodic with periods 12, 20, and 28. The structure of the orbits of periodic tiles is as follows, see Figure 10.

- One orbit consisting of the tiles that return to themselves after 3 iterations, with the return map having order 4.
- One orbit consisting of the tiles that return to themselves after 10 iterations, with the return map having order 2.
- One orbit consisting of the tiles that return to themselves after 20 iterations, with the return map being the identity.
- One orbit consisting of the tiles that return to themselves after 7 iterations, with the return map having order 4.
- Two orbits consisting of the tiles that return to themselves after 28 iterations, with the return map being the identity.

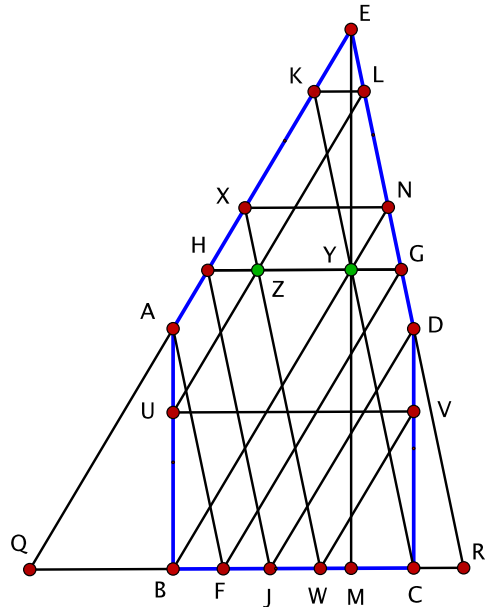


Figure 11. *Marked tall Penthouse.*

In the first bifurcation case when m changes values from 1 to 2, i.e., for $a = 1$, the billiard map is fully periodic with one period being 28, see Figure 10. This is consistent with Conjecture 4.1. We point out that there are three different types of symbolic orbits, though.

Proof. The following proof relies on Figure 11. Without loss of generality, we assume that $b > 1/2$, that is, vertex E is right of the perpendicular bisector of side BC . In this figure, the lines are parallel to the sides of the pentagon. If vertex E moves horizontally, the order of some points on side BC may change.

For our analysis, it is important to notice two concurrences of lines, at points Y and Z . Let us prove this elementary geometry fact for point Y ; point Z is treated similarly. We also note that $EK = XH$, $EL = NG$, and hence $HZ = YG$; this will follow from the analysis of the dynamics below.

Let Y be the intersection point of the lines BN and CK . First we show that the perpendicular, dropped from E to the base BC , passes through Y . Indeed, since $ABCD$ is a square, the triangle AED is obtained from the triangle BYC by the vertical parallel translation. Therefore the altitude from vertex Y is translated to the altitude from vertex E , hence they lie on the same vertical line.

Next, let HG be the horizontal segment through point Y . Draw the line parallel to EA through point G to construct point F , and then the line parallel to ED through point F . We need to show that this line passes through the vertex of the square, point A .

Indeed, let A' be the intersection of this line with the vertical line through point B . We want to show that $A' = A$. We have $BF = YG = CR$, hence the triangles CDR and $BA'F$ are congruent, and therefore $A' = A$.

A similar argument shows that if one draws the line parallel to ED through point H to construct point J , and then the line parallel to EA through point J , then this line passes through vertex D .

Now we can describe the evolution of phase rectangles. We refer to Figure 11. For a point on the “roof”, such as point X , we use the notation X^\perp for its orthogonal projection on the base BC (these projections are not marked not to clutter the figure).

The 3-periodic orbit is easy to describe, it consists of the tiles surrounding the 3-periodic orbit in triangle QER that connects the midpoints of its sides:

$$(2) \quad HA \times FJ \rightarrow FJ \times DG \rightarrow DG \times HA \rightarrow HA \times FJ.$$

The 10-periodic orbit is as follows:

$$(3) \quad \begin{aligned} NL \times HA &\rightarrow HA \times UB \rightarrow UB \times BH^\perp \rightarrow BH^\perp \times CV \rightarrow CV \times HA \rightarrow \\ HA \times WC &\rightarrow WC \times DG \rightarrow DG \times KX \rightarrow KX \times FJ \rightarrow FJ \times NL \rightarrow NL \times HA. \end{aligned}$$

The 7-periodic orbit is as follows:

$$(4) \quad \begin{aligned} NL \times KX &\rightarrow KX \times UB \rightarrow UB \times X^\perp K^\perp \rightarrow X^\perp K^\perp \times CV \rightarrow \\ CV \times KX &\rightarrow KX \times WC \rightarrow WC \times NL \rightarrow NL \times KX. \end{aligned}$$

Here is a 20-periodic orbit:

$$(5) \quad \begin{aligned} LE \times HA &\rightarrow HA \times AU \rightarrow AU \times BH^\perp \rightarrow BH^\perp \times VD \rightarrow VD \times HA \rightarrow \\ HA \times JW &\rightarrow JW \times DG \rightarrow DG \times XH \rightarrow XH \times FJ \rightarrow FJ \times GN \rightarrow \\ GN \times HA &\rightarrow HA \times BF \rightarrow BF \times DG \rightarrow DG \times AB \rightarrow AB \times G^\perp C \rightarrow \\ G^\perp C \times CD &\rightarrow CD \times DG \rightarrow DG \times EK \rightarrow EK \times FJ \rightarrow FJ \times LE \rightarrow LE \times HA. \end{aligned}$$

It remains to describe the two 28-periodic orbits. Here they are:

$$(6) \quad \begin{aligned} LE \times EK &\rightarrow EK \times AU \rightarrow AU \times K^\perp E^\perp \rightarrow K^\perp E^\perp \times VD \rightarrow VD \times EK \rightarrow \\ EK \times JW &\rightarrow JW \times LE \rightarrow LE \times XH \rightarrow XH \times AU \rightarrow AU \times H^\perp X^\perp \rightarrow \\ H^\perp X^\perp \times VD &\rightarrow VD \times XH \rightarrow XH \times JW \rightarrow JW \times GN \rightarrow GN \times XH \rightarrow \\ XH \times BF &\rightarrow BF \times GN \rightarrow GN \times AB \rightarrow AB \times N^\perp G^\perp \rightarrow N^\perp G^\perp \times CD \rightarrow \\ CD \times GN &\rightarrow GN \times EK \rightarrow EK \times BF \rightarrow BF \times LE \rightarrow LE \times AB \rightarrow \\ AB \times E^\perp L^\perp &\rightarrow E^\perp L^\perp \times CD \rightarrow CD \times LE \rightarrow LE \times EK, \end{aligned}$$

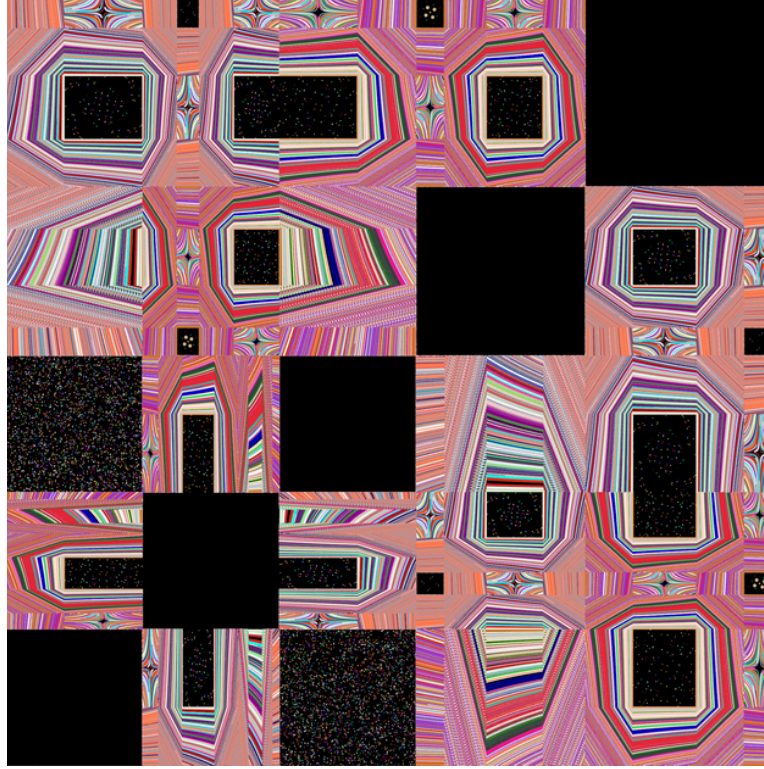


Figure 12. *The phase portrait of a small perturbation of a tall Penthouse: in accordance with Proposition 2.1, the 3- and 7-periodic orbits survive the perturbation.*

and

$$\begin{aligned}
 (7) \quad NL \times EK &\rightarrow EK \times UB \rightarrow UB \times K^\perp M \rightarrow K^\perp M \times CV \rightarrow CV \times EK \rightarrow \\
 &EK \times WC \rightarrow WC \times LE \rightarrow LE \times KX \rightarrow KX \times AU \rightarrow AU \times X^\perp K^\perp \rightarrow \\
 &X^\perp K^\perp \times VD \rightarrow VD \times KX \rightarrow KX \times JW \rightarrow JW \times NL \rightarrow NL \times XH \rightarrow \\
 &XH \times UB \rightarrow UB \times H^\perp X^\perp \rightarrow H^\perp X^\perp \times CV \rightarrow CV \times XH \rightarrow XH \times WC \rightarrow \\
 &WC \times GN \rightarrow GN \times KX \rightarrow KX \times BF \rightarrow BF \times NL \rightarrow NL \times AB \rightarrow \\
 &AB \times L^\perp N^\perp \rightarrow L^\perp N^\perp \times CD \rightarrow CD \times NL \rightarrow NL \times EK.
 \end{aligned}$$

By inspection, the above described orbits cover the whole phase space. Therefore, it remains to consider the case $a = 1$.

In the limit $a \searrow 1$ the tiles with sides HA , FJ , and DG disappear simultaneously. This kills the periodic orbits (2), (3), and (5). At the same time the periodic orbits (4), (6), and (7) survive. Their tiles still cover the phase space and they give rise to different symbolic orbits. \square

The next Figure 12 shows the phase space of a small perturbation of a tall Penthouse.

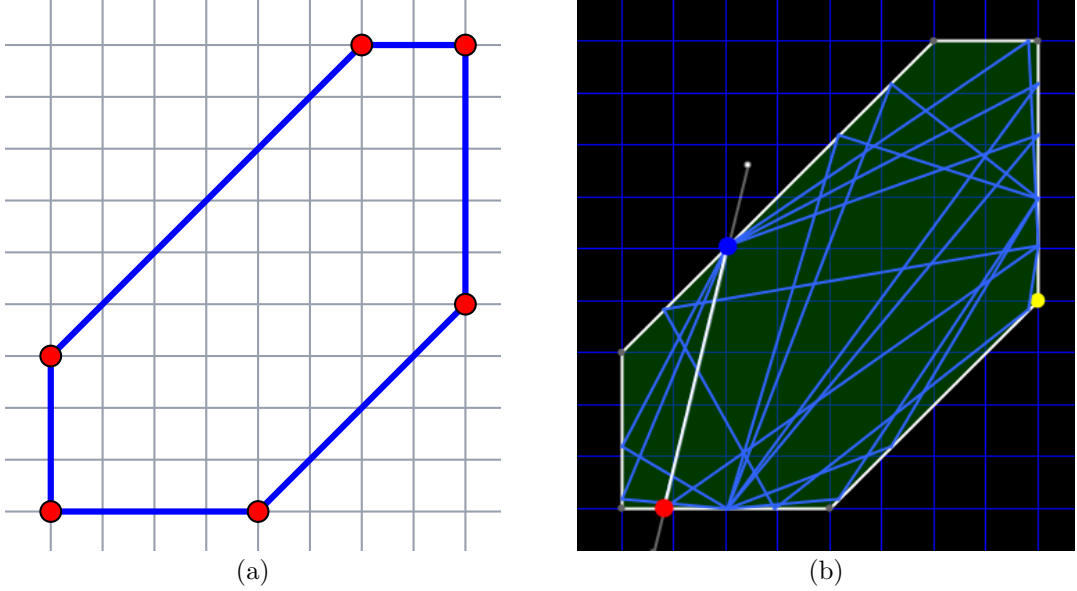


Figure 13. A lattice hexagon with parallel opposite sides (a) and a corresponding periodic orbit (b).

5. (LATTICE) HEXAGONS WITH PARALLEL OPPOSITE SIDES

We first consider hexagons with parallel opposite sides. After an affine transformation we assume that the directions of the sides are those of an equilateral triangle. In this situation we have the following immediate corollary of Lemma 2.1.

Corollary 5.1. *Let P be a hexagon as above. The symplectic billiard map T is a local Euclidean isometry and has the form*

$$T : (x, y) \mapsto (y, -x + b), \quad x \in P_i P_{i+1}, y \in P_j P_{j+1}, z \in P_k P_{k+1},$$

where b depends on i, j, k . In particular, the symplectic billiard map T has no hyperbolic periodic points.

Remark 5.1. The affine invariant version of the previous corollary is that for any hexagon with parallel opposite sides the symplectic billiard map is a local isometry with respect to inner product AA^t , where A relates the given hexagon with a hexagon from Corollary 5.1.

We also point out that, as opposed to Remark 2.1, in this special situation T is a isometry with respect to a sign-definite inner product, e.g., leading to the strong conclusion that it doesn't admit hyperbolic periodic points.

A hexagon with parallel opposite sides is obtained from a triangle by cutting off the corners by the lines parallel to the sides. Applying an affine transformation, we may assume that the slopes of the sides are equal to 0, 1 and ∞ . In addition, we now consider lattice polygons, i.e, all vertices are lattice points, see Figure 13. The affine moduli space of these hexagons is described by three integral parameters (whereas the affine moduli space of hexagons is 6-dimensional).

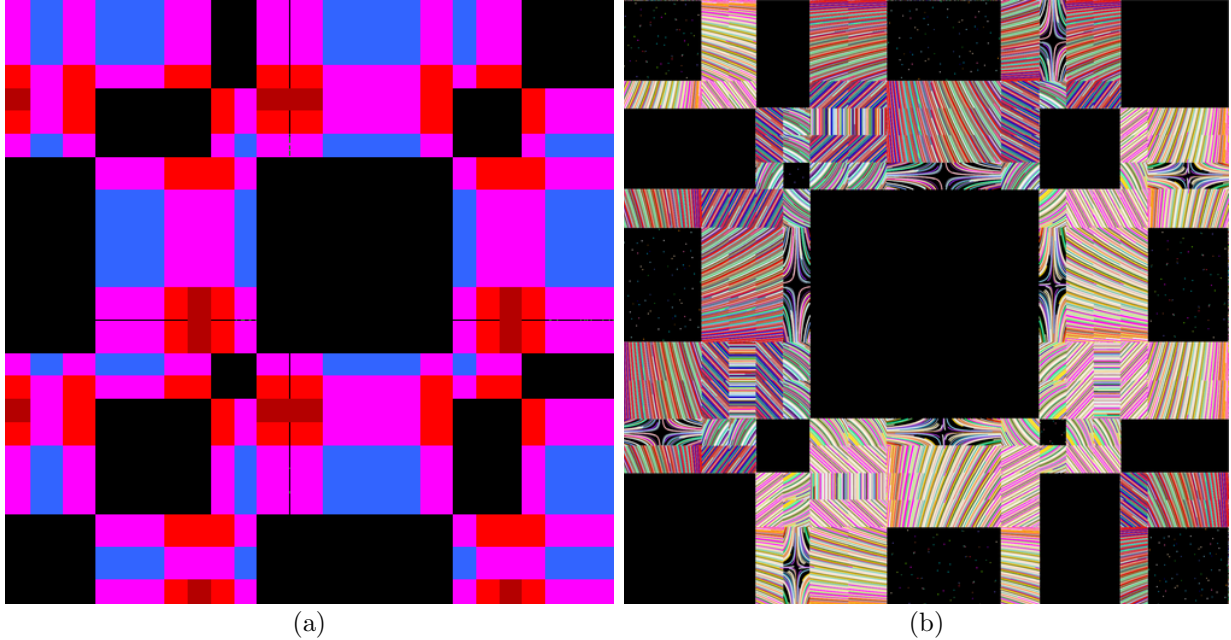


Figure 14. The phase space (a) of the hexagon from Figure 13: the periods are 4, 12, 24, 36. The phase space (b) of a small perturbation of the same hexagon.

The lattice points partition the sides into segments; let $p_1, q_1, r_1, p_2, q_2, r_2$ be the number of these elementary segments on the six sides in the cyclic order. Set

$$N = p_1 q_1 + q_1 r_1 + r_1 p_2 + p_2 q_2 + q_2 r_2 + r_2 p_1 + p_1 r_1 + q_1 p_2 + r_1 q_2 + p_2 r_2 + q_2 p_1 + r_2 q_1.$$

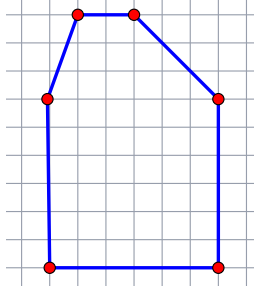
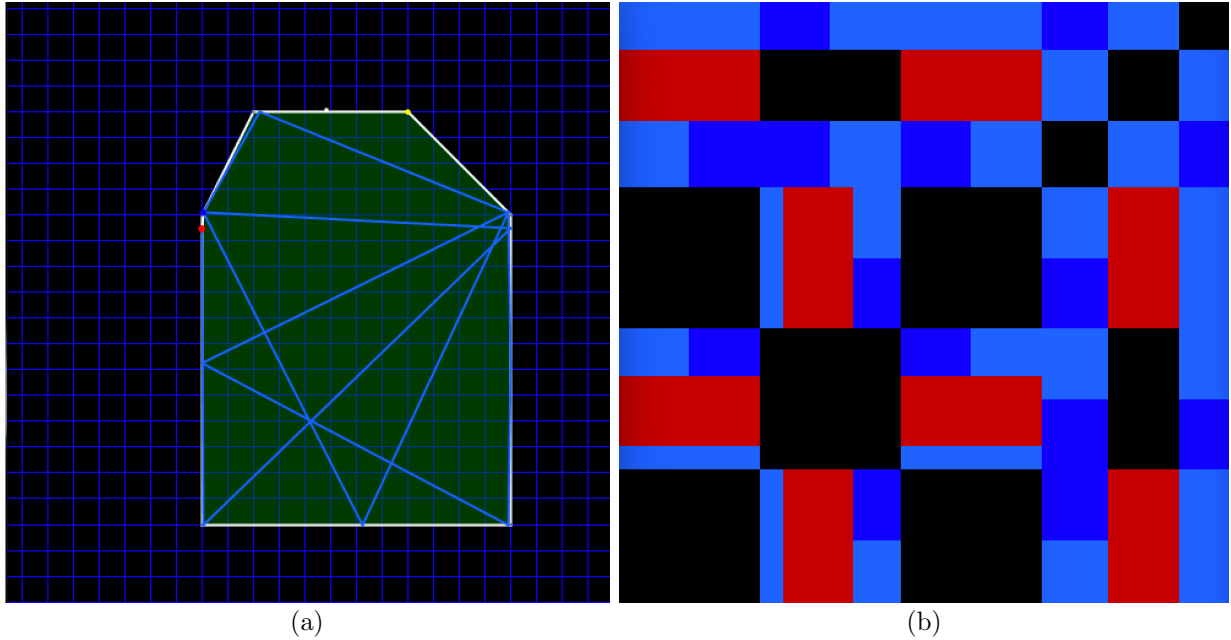
Theorem 5.1. All orbits in a lattice hexagon with parallel opposite sides are periodic, and the periods do not exceed $4N$.

Proof. The phase space is subdivided into the tiles formed by the products of the elementary segments on the sides, that is, segments between lattice points, see Figure 13. These tiles evolve as single pieces under the symplectic billiard map. The phase area of each tile is one, and the whole phase area equals N . By the area preserving property, the period of the orbit of each tile does not exceed N , and the return map to a tile is at most 4-periodic. \square

Of course, the upper bound of this theorem is unrealistically high. See Figure 13 for an example of an orbit and Figure 14 for the phase space, colored according to periods.

The next Figure 14 shows the phase portrait of a small perturbation of a hexagon with parallel opposite sides.

Remark 5.2. Consider a hexagon P with parallel opposite sides having rational slopes. One can approximate P by a rational hexagon whose vertices have rational coordinates. The symplectic billiard orbits in the approximating polygons are periodic, but their periods will grow with the least common denominators of the coordinates of the vertices of the approximating polygons. The same applies to the polygons described in the next section.

**Figure 15.** A hex(en)house.**Figure 16.** A periodic Hexhouse with periods 4, 12, 28.

6. THE HEX(EN)HOUSE AND SPECIAL OCTAGONS

In this section we present two more families with fully periodic symplectic billiard map, the hex(en)house and special octagons. We can only give computer evidence and formulate two corresponding conjectures.

The Hexhouse is a lattice polygon obtained by placing a trapezoid on top of a square, see Figure 15. The moduli space of such polygons is described by three integral parameters. Figures 16–19 support the following conjecture. Figure 20 shows again the typical pattern of a perturbation.

Conjecture 6.1. *All orbits in a Hexhouse are periodic.*

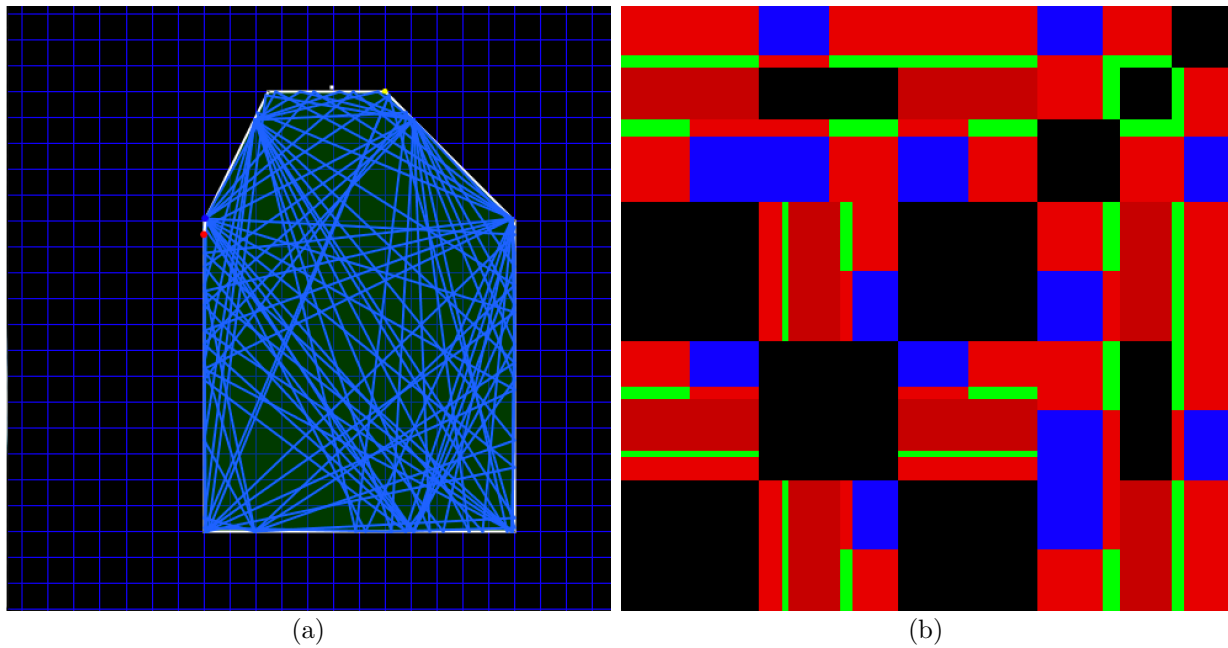


Figure 17. Another periodic Hexhouse with periods 4, 28, 108, 188.

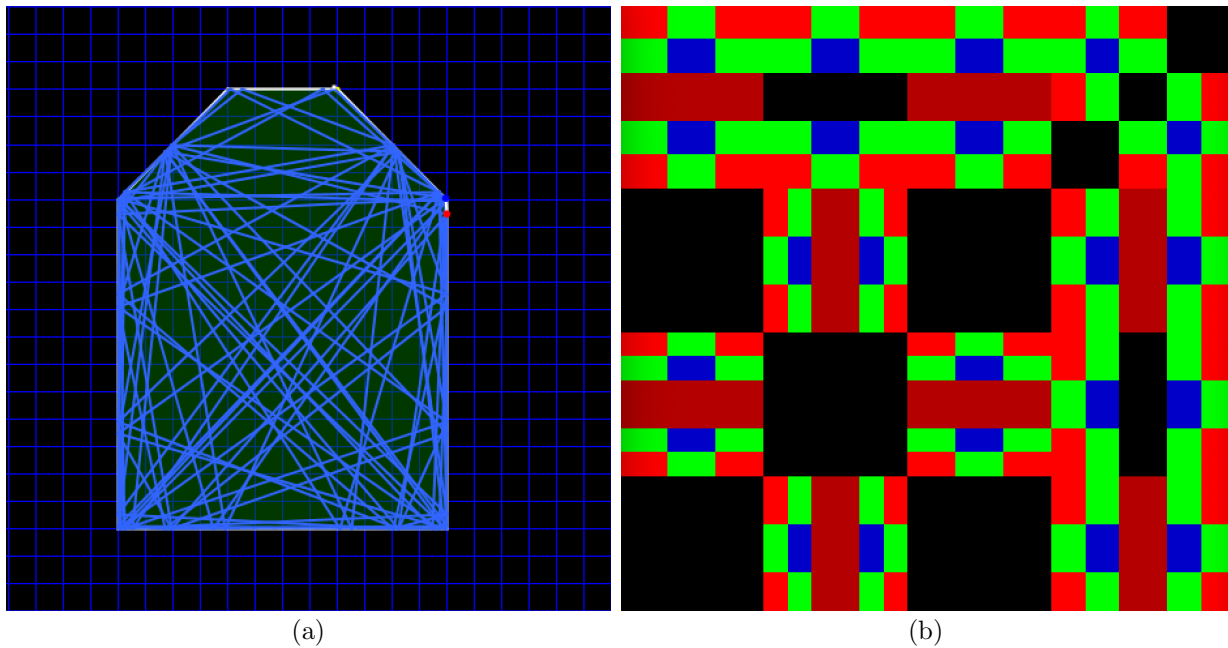


Figure 18. Yet another periodic Hexhouse with periods 4, 44, 68, 92.

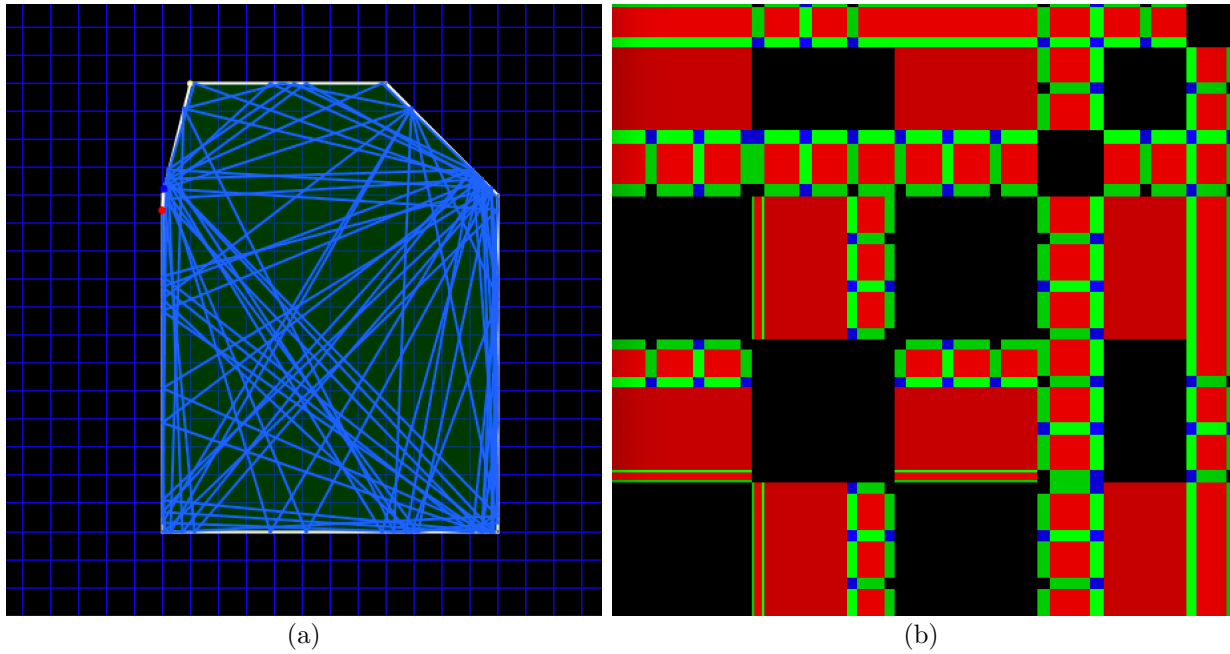


Figure 19. *The last periodic Hexhouse, periods are 4, 28, 44, 60, 68, 84, 108.*

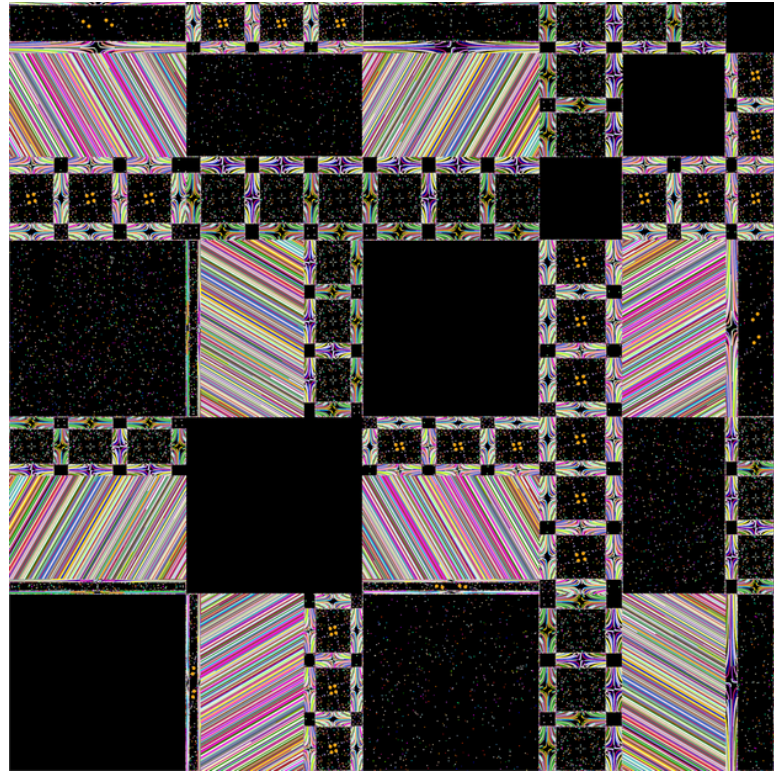


Figure 20. *A small perturbation of the previous Hexhouse.*

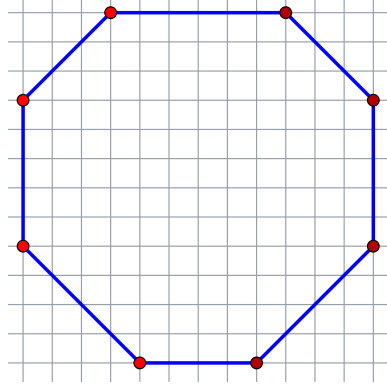


Figure 21. *A special octagon.*

Special octagons are lattice octagons whose opposite sides are parallel and have slopes $0, \pm 1, \infty$, and that have an axis of symmetry parallel to a pair of sides, see Figure 21. Their symmetries are dilations and translations in \mathbf{R}^2 . The corresponding moduli space is 3-dimensional over the integers since we only consider lattice octagons. This can be seen as follows. Fix a rectangle with vertical and horizontal sides centered at the origin. Then cut off two corners with diagonal lines and cut the other two corners according to symmetry. These are four-dimensional choices which after dividing out dilations give rise to a three dimensional moduli space.

Figures 22 and 23 show two pictures as evidence for the following conjecture, and Figure 24 again the typical pattern caused by a perturbation.

Conjecture 6.2. *All orbits in a special octagon are periodic.*

7. OPEN PROBLEMS AND CONJECTURES

An outstanding open problem concerning (Euclidean) polygonal billiards is whether they always have a periodic orbit. This is not known even for obtuse triangles (the acute and right triangles possess periodic orbits). The current state of the art is that all obtuse triangles with the angles not exceeding 112.3 degrees have periodic billiard trajectories, [2, 5]. In contrast, all polygonal outer billiards possess periodic orbits, [4].

Question 7.1. *Do all polygonal symplectic billiards have periodic trajectories?*

This is particularly intriguing since a computer search on the kites with corners given by $(-1, 1), (-1, -1), (1, -1), (3, 3)$ did not find a periodic orbit of period less than 2000. This is the “smallest” lattice kite not being a square.

Acknowledgements. This work is supported by Deutsche Forschungsgemeinschaft (DFG) under Germany’s Excellence Strategy EXC-2181/1 - 390900948 (the Heidelberg STRUCTURES Excellence Cluster) and by the Transregional Collaborative Research Center SFB / TRR 191, NSF grant DMS-1510055, the Interdisciplinary Center for Scientific Computing (IWR), and HGS MathComp.

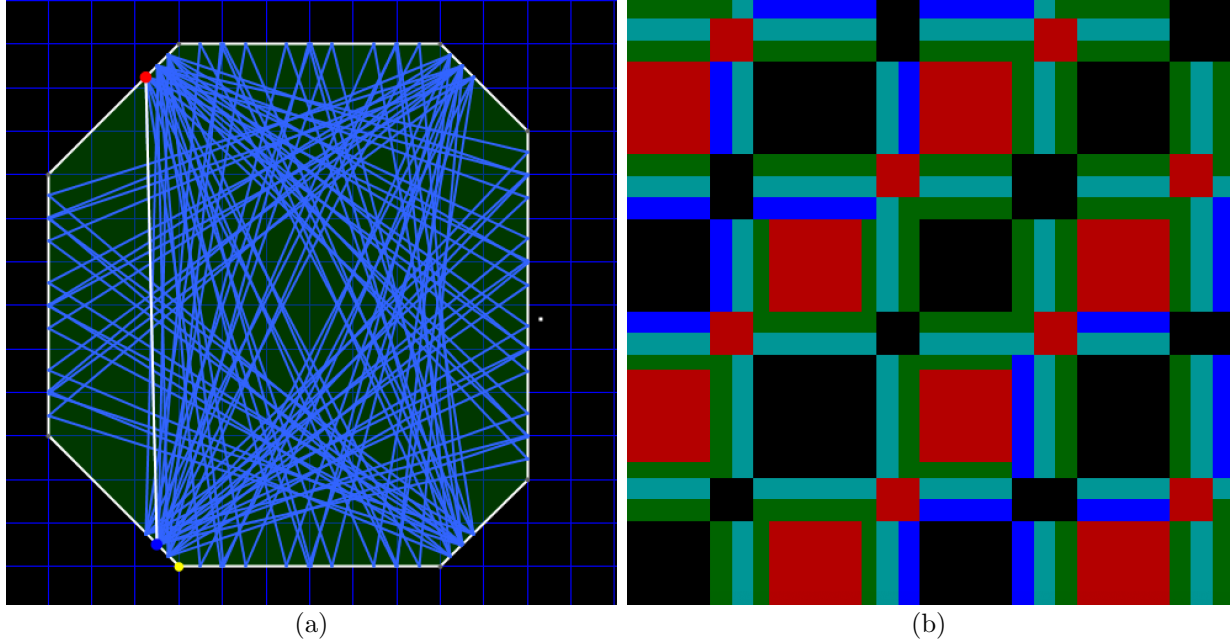


Figure 22. A periodic special octagon with periods: 4, 56, 68, 108.

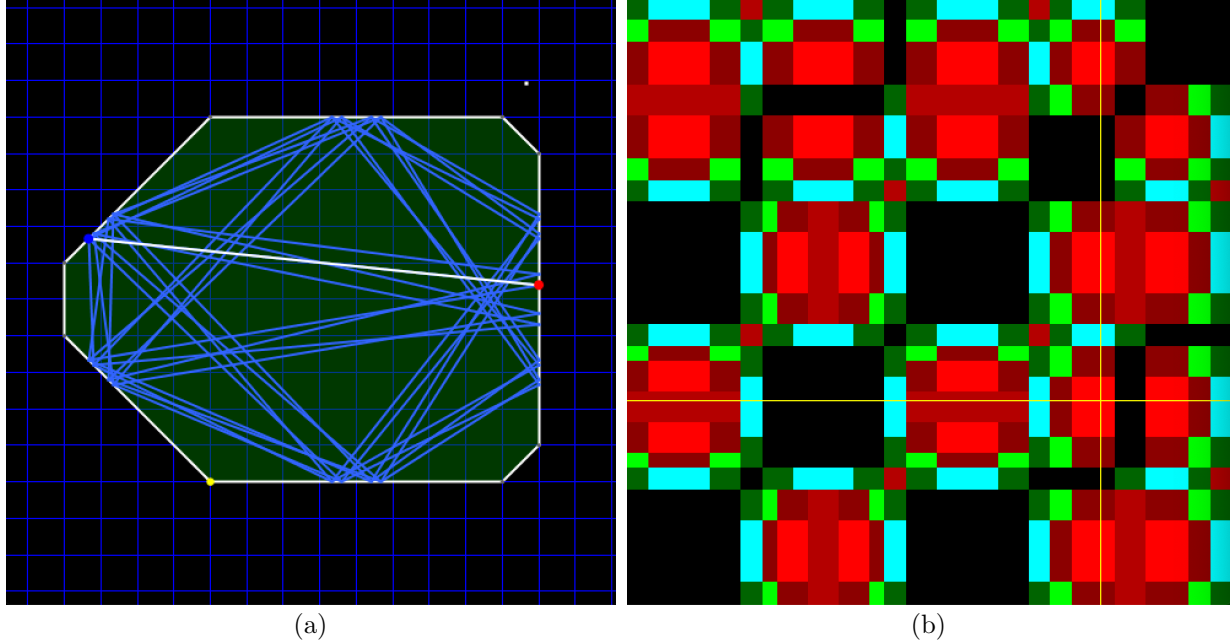


Figure 23. A second periodic special octagon with periods: 4, 16, 32, 44, 68, 92.

We also would like to thank Lutz Hofmann and Peter Hügel for their technical support and contributions, and respective funding within the subproject A7 of the Transregional Collaborative Research Center SFB / TRR 165.

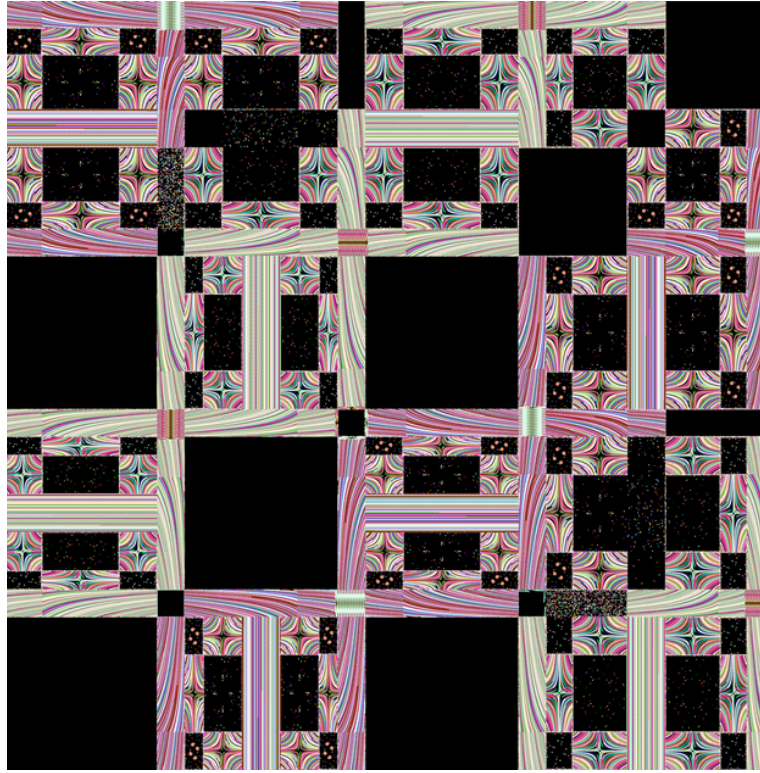


Figure 24. *A small perturbation of the previous special octagon.*

REFERENCES

- [1] P. Albers, S. Tabachnikov. *Introducing symplectic billiards*. Advances in Math. **333** (2018), 822–867.
- [2] R. Schwartz. *Obtuse triangular billiards. II. One hundred degrees worth of periodic trajectories*. Experiment. Math. **18** (2009), 137–171.
- [3] S. Tabachnikov. *Geometry and billiards*. Amer. Math. Soc., Providence, RI, 2005.
- [4] S. Tabachnikov. *A proof of Culter's theorem on the existence of periodic orbits in polygonal outer billiards*. Geom. Dedicata **129** (2007), 83–87.
- [5] G. Tokarsky, J. Garber, B. Marinov, K. Moore. *One hundred and twelve point three degree theorem*. arXiv:1808.06667.
- [6] S. Boshe-Plois, Q. Q. Ngo, P. Albers, L. Linsen. *Visual analysis of billiard dynamics simulation ensembles*. Proceedings of International Conference on Information Visualization Theory and Applications (IVAPP), to appear.

PETER ALBERS, MATHEMATISCHES INSTITUT AND INTERDISCIPLINARY CENTER FOR SCIENTIFIC COMPUTING (IWR), RUPRECHT-KARLS-UNIVERSITÄT HEIDELBERG, GERMANY
E-mail address: peter.albers@uni-heidelberg.de

GAUTAM BANHATTI, MATHEMATISCHES INSTITUT, RUPRECHT-KARLS-UNIVERSITÄT HEIDELBERG, GERMANY
E-mail address: gautam@posteo.de

FILIP SADLO, INTERDISCIPLINARY CENTER FOR SCIENTIFIC COMPUTING (IWR), RUPRECHT-KARLS-UNIVERSITÄT HEIDELBERG, GERMANY

E-mail address: `sadlo@uni-heidelberg.de`

RICHARD SCHWARTZ, DEPARTMENT OF MATHEMATICS, BROWN UNIVERSITY, USA

E-mail address: `res@math.brown.edu`

SERGE TABACHNIKOV, DEPARTMENT OF MATHEMATICS, PENNSYLVANIA STATE UNIVERSITY, USA

E-mail address: `tabachni@math.psu.edu`